Scaling Theory for Mechanical Critical Behavior in Fiber Networks

Jordan L. Shivers, Sadjad Arzash, Abhinav Sharma, and Fred C. MacKintosh

Scaling theory for mechanical critical behavior in fiber networks

Jordan L. Shivers,[1, 2] Sadjad Arzash,[1, 2] Abhinav Sharma,[3] and Fred C. MacKintosh[1, 2, 4]

[1]*Department of Chemical and Biomolecular Engineering, Rice University, Houston, TX 77005, USA*
[2]*Center for Theoretical Biological Physics, Rice University, Houston, TX 77030, USA*
[3]*Leibniz Institute of Polymer Research Dresden, Dresden, Germany*
[4]*Departments of Chemistry and Physics & Astronomy, Rice University, Houston, TX 77005, USA*

As a function of connectivity, spring networks exhibit a critical transition between floppy and rigid phases at an isostatic threshold. For connectivity below this threshold, fiber networks were recently shown theoretically to exhibit a rigidity transition with corresponding critical signatures as a function of strain. Experimental collagen networks were also shown to be consistent with these predictions. We develop a scaling theory for this strain-controlled transition. Using a real-space renormalization approach, we determine relations between the critical exponents governing the transition, which we verify for the strain-controlled transition using numerical simulations of both triangular lattice-based and packing-derived fiber networks.

It has long been recognized that varying connectivity can lead to a rigidity transition in networks such as those formed by springlike, central force (CF) connections between nodes. Maxwell introduced a counting argument for the onset of rigidity for such systems in d dimensions with N nodes, in which the number of degrees of freedom dN is balanced by the number of constraints $Nz/2$, where z is the average coordination number of the network [1]. The transition at this *isostatic* point of marginal stability has been shown to exhibit signatures of criticality. Such a balance of constraints and degrees of freedom is important for understanding rigidity percolation and jamming [2–6]. Even in networks with additional interactions that lead to stability below the CF isostatic point, the mechanical response can still exhibit strong signatures of criticality in the vicinity of the CF isostatic point [7–10]. More recently, criticality has been shown in fiber networks as a function of strain for systems well below the isostatic point [11].

While both jammed particle packings and fiber networks exhibit athermal ($T = 0$) mechanical phase transitions and superficially similar critical behavior, these systems have strong qualitative differences. In particular, there is growing evidence that the jamming transition is mean-field [6, 12]. Goodrich et al. recently proposed a scaling theory and performed numerical simulations of jamming which both demonstrate mean-field exponents and support the conclusion that the upper critical dimension $d_u = 2$ for the jamming transition [12]. In contrast, fiber networks to date have shown distinctly non-mean-field behavior [8–11]. Although many aspects of the critical behavior of fiber networks, including various critical exponents, have been quantified, prior studies have been limited to to simulations and the development of effective medium theories. Importantly, a theory has been lacking to identify critical exponents or even scaling relations among exponents, in order to understand the observed non-mean-field character of the stiffening transition in fiber networks. Here, we develop a scaling theory for both the sub-isostatic, strain controlled transition, as well as the transition in z near the isostatic point for athermal fiber networks. We derive scaling relations among the various exponents and demonstrate good agreement with numerical simulations. Interestingly, our re-

sults imply that the upper critical dimension for fiber networks is $d_u > 2$, in contrast with jamming packings.

Near the isostatic point with average coordination number $z = z_c = 2d$, spring networks exhibit linear shear moduli G that vary as a power of $|z - z_c|$ for $z > z_c$ [6, 7, 13]. In the floppy or sub-isostatic regime with $z < z_c$, such systems can be stabilized by introducing additional interactions [7, 8] or by imposing stress or strain [14, 15]. It was recently shown that sub-isostatic networks undergo a transition from floppy to rigid as a function of shear strain γ [11, 16]. Moreover, this fundamentally nonlinear transition was identified as a line of critical points characterized by a z−dependent threshold $\gamma_c(z)$, as sketched in Fig. 1a. Above this strain threshold, the differential or tangent shear modulus $K = d\sigma/d\gamma$ scales as a power law in strain, with $K \sim |\gamma - \gamma_c|^f$. Introducing bending interactions with rigidity κ between nearest neighbor bonds stabilizes sub-isostatic networks below the critical strain, leading to $K \sim \kappa$ for $\gamma < \gamma_c$. Both of these regimes are captured by the scaling form [17]

$$K \approx |\gamma - \gamma_c|^f \, \mathcal{G}_\pm \left(\kappa/|\gamma - \gamma_c|^\phi \right) \qquad (1)$$
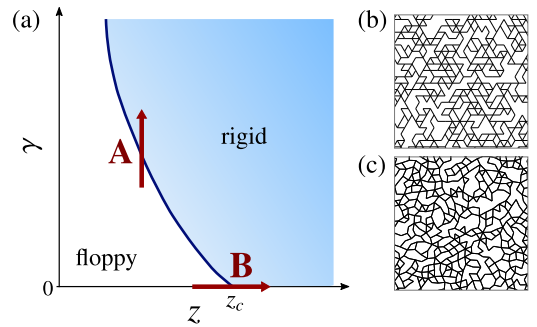

FIG. 1. (a) Schematic phase diagram depicting the state of mechanical rigidity of a central force network as a function of coordination number z and applied shear strain γ. The arrow A depicts the strain-controlled transition and B depicts the transition at the isostatic point. With the addition of bending interactions, the floppy region becomes instead bending-dominated, but the critical curve $\gamma_c(z)$ vs. z remains the same. (b) Portion of a a triangular network and (c) a 2D packing-derived network, both diluted to $z = 3.3 < z_c$.

for $\kappa > 0$, in which the branches of the scaling function $\mathcal{G}_\pm$ account for the strain regimes above and below γ_c. This scaling form was also shown to successfully capture the nonlinear strain stiffening behavior observed in experiments on reconstituted networks of collagen, a filamentous protein that provides mechanical rigidity to tissues as the primary structural component of the extracellular matrix [16]. Collagen constitutes an excellent experimental model system on which to study this transition, as it forms elastic networks that are deeply sub-isostatic ($z \approx 3.4$ [18], whereas $z_c = 6$ in 3D) in which individual fibrils have sufficiently high bending moduli to be treated as athermal elastic rods.

Scaling theory — For the strain-controlled transition at a fixed $z < z_c$ (arrow A in Fig. 1a), we define a reduced variable $t = \gamma - \gamma_c$ that vanishes at the transition and let $h(t, \kappa)$ denote the Hamiltonian or elastic energy per unit cell. This energy depends on the bending stiffness κ that also vanishes at the transition. Assuming the system becomes critical as $t, \kappa \to 0$, we consider the real-space renormalization of the system when scaled by a factor L to form a block or effective unit cell composed of L^d original cells, where d is the dimensionality of the system [19]. Under this transformation, the energy per block becomes $h(t', \kappa') = L^d h(t, \kappa)$, where t' and κ' are renormalized values of the respective parameters. We assume that the parameters evolve according to $t \to t' = tL^x$ and $\kappa \to \kappa' = \kappa L^y$, where the exponents x, y can be assumed to be positive, since the system must evolve away from criticality. Combining these, we find the elastic energy

$$h(t, \kappa) = L^{-d} h(tL^x, \kappa L^y). \tag{2}$$

The stress is simply given by the derivative with respect to strain of the elastic energy per volume, which is proportional to $h(t, \kappa)$. Thus, $\sigma \sim \frac{\partial}{\partial \gamma} h \sim \frac{\partial}{\partial t} h(t, \kappa) \sim L^{-d+x} h_{1,0}(tL^x, \kappa L^y)$ and the stiffness

$$K = \frac{\partial}{\partial \gamma} \sigma \sim \frac{\partial^2}{\partial t^2} h(t, \kappa) \sim L^{-d+2x} h_{2,0}(tL^x, \kappa L^y), \tag{3}$$

where $h_{n,m}$ refers to the combined n-th partial with respect to t and m-th partial with respect to κ of h. Being derivatives of the energy with respect to the control variable γ, the stress and stiffness are analogous to the entropy and heat capacity for a thermal system with phase transition controlled by temperature. If we let $L = |t|^{-1/x}$, then the correlation length scales according to $\xi \sim L \sim |t|^{-\nu}$, from which we can identify the correlation length exponent $\nu = 1/x$. Thus, the stiffness can be expressed as in Eq. (1), where $\mathcal{G}_\pm(s) \sim h_{2,0}(\pm 1, s)$ and

$$f = d\nu - 2 \quad \text{and} \quad \phi = y\nu. \tag{4}$$

The first of these is a hyperscaling relation analogous to that for the heat capacity exponent for thermal critical phenomena, but with the opposite sign. Thus, $f > 0$ corresponds to nonlinear stiffness K that is non-divergent. For $\gamma > \gamma_c$, we expect that $h_{2,0}(1, s)$ is approximately constant for $s \ll 1$, so that $K \sim |\gamma - \gamma_c|^f$, while for $\gamma < \gamma_c$ we expect that $h_{2,0}(-1, s) \sim s$

for $s \ll 1$, so that

$$K \sim \kappa |\gamma - \gamma_c|^{-\lambda}, \tag{5}$$

consistent with a bending-dominated regime. Moreover, the susceptibility-like exponent is expected to be $\lambda = \phi - f$.

Near the critical strain, athermal networks exhibit large, nonaffine internal rearrangements in response to small changes in applied strain [11, 16]. These nonaffine strain fluctuations are analogous to divergent fluctuations in other critical systems. In response to an incremental strain strain step $\delta\gamma$, the nonaffine displacement of the nodes is expected to be proportional to $\delta\gamma$. Thus, the nonaffine fluctuations can be captured by $\delta\Gamma \sim \langle |\delta\mathbf{u} - \delta\mathbf{u}^A|^2 \rangle / \delta\gamma^2$, where $\delta\mathbf{u} - \delta\mathbf{u}^A$ represents the deviation relative to a purely affine displacement $\delta\mathbf{u}^A$. For large systems with small κ, $\delta\Gamma$ diverges as $t \to 0$ [16]. Since the nonaffine displacements δu^2 are determined by the minimization of $h(t, \kappa)$, for small κ, $h \sim \kappa \delta u^2 \sim \kappa \delta\gamma^2 \delta\Gamma$. Thus, the nonaffine fluctuations are predicted to diverge as

$$\delta\Gamma \sim \frac{\partial}{\partial \kappa} \frac{\partial^2}{\partial t^2} h(t, \kappa) \sim |t|^{-\lambda}, \tag{6}$$

with the same exponent $\lambda = \phi - f$ as in Eq. (5).

Computational model — To test the scaling relations derived above, we study two complementary models of fiber networks: triangular lattice-based networks and jammed packing-derived networks. Our triangular networks consist of fibers of length W arranged on a periodic triangular lattice with lattice spacing $l_0 = 1$, with freely-hinging crosslinks attaching overlapping fibers. To avoid system-spanning straight fibers, we initially cut a single randomly chosen bond on each fiber, yielding an initial network coordination number z approaching 6 from below with increasing W [8, 20]. We prepare packing-derived networks by populating a periodic square unit cell of side length W with $N = W^2$ randomly placed, frictionless bidisperse disks with soft repulsive interactions and with a ratio of radii of 1 : 1.4. The disks are uniformly expanded until the point at which the system develops finite bulk and shear moduli, after which a contact network excluding rattlers is generated [6, 21, 22]. Sufficiently large networks prepared using this protocol have an initial connectivity $z \approx z_c$ [23].

For both network structures, we reduce z to a value below the isostatic threshold by bond dilution and removal of dangling ends [24]. We use a random dilution process, in contrast with special cutting protocols that have been used previously to suppress variation in local connectivity and promote meanfield behavior [7, 25]. Unless otherwise stated, we use triangular networks of size $W = 140$ and packing-derived networks of size $W = 120$, both with $z = 3.3$, and simulate ensembles of at least 30 network realizations each. Sample network structures are shown in Fig. 1b-c.

We treat each bond as a Hookean spring with 1D modulus μ, such that the contribution of stretching to the network

energy is

$$\mathcal{H}_S = \frac{\mu}{2} \sum_{\langle ij \rangle} \frac{\left(l_{ij} - l_{ij,0}\right)^2}{l_{ij,0}} \qquad (7)$$

in which l_{ij} and $l_{ij,0}$ are the length and rest length, respectively, of the bond connecting nodes i and j. Bending interactions are included between pairs of nearest-neighbor bonds, which are treated as angular springs with bending modulus κ. For triangular networks, bending interactions are only considered between pairs of bonds along each fiber, which are initially collinear, whereas for packing-derived networks we account for all nearest-neighbor bonds. The contribution of bending to the network energy is

$$\mathcal{H}_B = \frac{\kappa}{2} \sum_{\langle ijk \rangle} \frac{\left(\theta_{ijk} - \theta_{ijk,0}\right)^2}{l_{ijk,0}} \qquad (8)$$

in which θ_{ijk} and $\theta_{ijk,0}$ are the angle and rest angle, respectively, between bonds ij and jk, and $l_{ijk,0} = (l_{ij,0} + l_{jk,0})/2$. We set $\mu = 1$ and vary the dimensionless bending stiffness κ [26].

We apply incremental quasistatic simple shear strain steps using Lees-Edwards periodic boundary conditions [27], minimizing the total network energy $\mathcal{H} = \mathcal{H}_S + \mathcal{H}_B$ at each step using the FIRE algorithm [28]. We compute the stress tensor as

$$\sigma_{\alpha\beta} = -\frac{1}{A} \sum_i f_{i,\alpha} u_{i,\beta}. \qquad (9)$$

in which $\mathbf{u}_i$ is the position of node i, $\mathbf{f}_i$ is the total force acting on node i, and A is the area of the system [24, 29, 30]. For the triangular lattice, $A = (\sqrt{3}/2)W^2$, and for packing-derived networks, $A = W^2$. The differential shear modulus K is computed as $K = \partial\sigma_{xy}/\partial\gamma$. To symmetrize K, we shear each network in both the $\gamma > 0$ and $\gamma < 0$ directions. Figure 2a shows $K(\gamma)$ for triangular networks with varying bending rigidity.

Results — First, we consider the scaling of K as a function of strain near γ_c. We determine γ_c for individual samples as the strain corresponding to the onset of finite K in the CF ($\kappa = 0$) limit, and utilize the mean of the resulting distribution, $\langle\gamma_c\rangle$, for our scaling analysis. The γ_c distribution for triangular networks of size $W = 140$ is shown in Figure 2a. We observe that with increasing system size, the width of the γ_c distribution decreases [24]. The stiffness K exhibits a small discontinuity at γ_c for $\kappa = 0$, as shown in Fig. 2a, consistent with prior reports in similar networks [31, 32]. We note that this discontinuity is, however, consistent with the critical nature of the transition, since K is not an order parameter.

We then determine f from $K \sim |\gamma - \gamma_c|^f$ in the low-κ limit. We obtain a distribution of estimated f values using sample-specific K curves and γ_c values for networks with $\kappa = 0$, yielding an estimate of $f = 0.73 \pm 0.04$ for triangular networks, as shown in Fig. 2b with decreasing κ. Similarly, for packing-derived networks we find $f = 0.68 \pm 0.04$ [24]. We
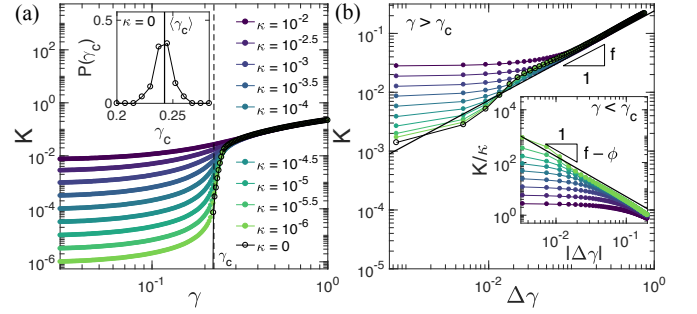

FIG. 2. (a) Differential shear modulus K vs. shear strain for triangular networks of connectivity $z = 3.3$, with varying reduced bending stiffness κ. The dashed line indicates the observed critical strain γ_c for the ensemble. The inset shows the probability distribution of γ_c for 50 individual network samples with $\kappa = 0$. (b) For $\gamma > \gamma_c$ and with decreasing κ, K converges to the form $K \sim |\gamma - \gamma_c|^f$, with $f = 0.73 \pm 0.04$. These data are for the same networks as in (a). Inset: In the low-κ limit and below γ_c, K/κ converges to a power law in $|\Delta\gamma|$ with exponent $f - \phi \approx -1.5$.

then estimate ϕ by averaging values computed from two separate scaling predictions, as follows. For $\gamma < \gamma_c$, we show the results for Eq. (5) in the inset to Fig. 2b. We also note that continuity of K as a function of strain near γ_c requires that $\mathcal{G}_\pm(s) \sim h_{2,0}(\pm 1, s) \sim s^{f/\phi}$ for large s. Thus, $K(\gamma_c) \sim \kappa^{f/\phi}$, as shown in the insets of Fig. 3a-b. Averaging the ϕ values computed from these corresponding fits, using our previously determined values for f, we estimate $\phi = 2.26 \pm 0.09$ for triangular networks and $\phi = 2.05 \pm 0.08$ for packing-derived networks. These values of f and ϕ are used in Figs. 3a-b, which demonstrate the collapse according to Eq. (1) [33].
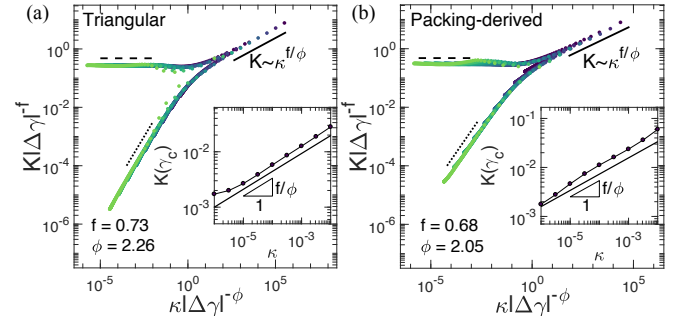

FIG. 3. Plotting the K vs. $|\Delta\gamma|$ data for both (a) triangular networks and (b) packing-derived networks according to the Widom-like scaling predicted by Eq. 1, and using the values of f and ϕ determined previously, yields a successful collapse for both systems. Dashed lines have slope 0 and dotted lines have slope 1. Insets: At the critical strain, $K \sim \kappa^{f/\phi}$.

We compute the nonaffine fluctuations $\delta\Gamma$ as

$$\delta\Gamma = \frac{1}{N l_c^2 \delta\gamma^2} \sum_i \|\delta\mathbf{u}_i^{NA}\|^2 \qquad (10)$$

in which N is the number of nodes, l_c is the average bond length, and $\delta\mathbf{u}_i^{NA} = \delta\mathbf{u}_i - \delta\mathbf{u}_i^A$ is the nonaffine component of

the displacement of node i due to the incremental strain $\delta\gamma$. Plotting $\delta\Gamma$ vs. $\gamma - \gamma_c$ in Fig. 4a, we observe agreement with the scaling predicted from Eq. (6) using the f and ϕ values determined above. Importantly, as predicted, the corresponding critical exponent $\lambda = \phi - f$ is the same as for Eq. (5), with $\lambda \simeq 1.5$ [34]. Further, we observe that near γ_c, the expected scaling $\delta\Gamma(\gamma_c) \sim \kappa^{f/\phi-1}$ appears to be satisfied [24].

It is apparent from Fig. 4a that the divergence of the fluctuations near γ_c is suppressed by finite-size effects. This is consistent with a diverging correlation length $\xi \sim |t|^{-\nu}$. Critical effects such as the divergence of $\delta\Gamma$ are limited as the correlation length becomes comparable to the system size W, corresponding to a value of $t \sim t_W = W^{-1/\nu}$. Thus, the maximum value of $\delta\Gamma$ increases as $\delta\Gamma \sim W^{(\phi-f)/\nu}$ (Fig. 4a inset). From least-squares fits to this scaling for both triangular and packing-derived networks with $\kappa = 0$ and $\kappa = 10^{-7}$, combined with our estimates for ϕ and f, we determine that $\nu = 1.3 \pm 0.2$ for both systems. We then verify that this leads to a scaling collapse in a plot of $\delta\Gamma W^{(f-\phi)/\nu}$ vs $tW^{1/\nu}$ for both systems with $\kappa = 0$, as shown in Fig. 4b, and with finite κ [24]. This finite-size scaling is consistent with the (hyperscaling-like) relation $f = 2\nu - 2$ in 2D from Eq. (4).
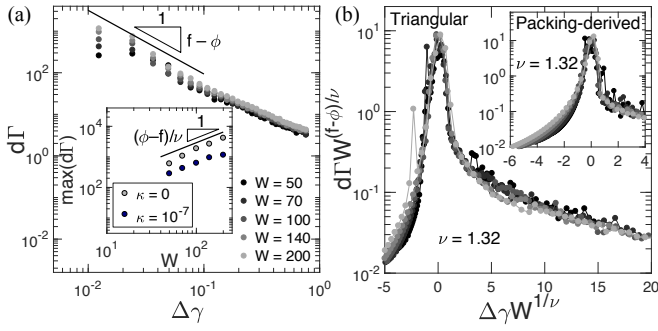

FIG. 4. (a) Near the critical strain, the nonaffinity scales as $\delta\Gamma \sim |\Delta\gamma|^{f-\phi}$. These data correspond to triangular networks with $\kappa = 10^{-7}$ and $z = 3.3$, with varying system size. Inset: Nonaffine fluctuations are limited by the system size. For small or zero κ, the maximum of $\delta\Gamma$ scales as $\max(\delta\Gamma) \sim W^{(\phi-f)/\nu}$, with $\nu = 1.3 \pm 0.2$. (b) Plots of $\delta\Gamma/W^{(\phi-f)/\nu}$ vs. $(\gamma - \gamma_c)W^{1/\nu}$ for triangular networks and (inset) packing-derived networks with $\kappa = 0$ demonstrate successful scaling collapse using the f and ϕ values determined from K, with ν values determined from the scaling relation.

Near the isostatic point — For networks near the isostatic transition at $z = z_c$, we define a dimensionless distance $\Delta = z - z_c$ from the isostatic point and let $h(\gamma, \kappa, \Delta)$ be the Hamiltonian or elastic energy per unit cell. At the isostatic point, since $\gamma_c = 0$, t above reduces to the strain γ. Assuming the system becomes critical as $\gamma, \kappa, \Delta \to 0$, we can follow a similar real-space renormalization procedure as above, resulting in

$$h(\gamma, \kappa, \Delta) = L^{-d} h(\gamma L^x, \kappa L^y, \Delta L^w). \quad (11)$$

Although the exponents x, y, and w at the isostatic point can be assumed to be positive, we do not necessarily assume the same values of the exponents x and y as determined for the

strain-controlled transition. We can again determine the stress σ and stiffness K as in Eq. (3). By letting $L = |\Delta|^{-1/w}$, we again identify the correlation length exponent $\nu' = 1/w$ and find

$$K \sim |\Delta|^{f'} h_{2,0,0}(0, \kappa/|t|^{\phi'}, \pm 1), \quad (12)$$

where

$$f' = (d - 2x)\nu', \quad \phi' = y\nu'. \quad (13)$$

Moreover, following similar arguments as above, it can be shown that $\delta\Gamma \sim |\Delta|^{-\lambda'}$, where $\lambda' = \phi' - f'$ [24, 35], consistent with the values $f' \simeq 1.4 \pm 0.1$, $\phi' \simeq 3.0 \pm 0.2$, $\nu' \simeq 1.4 \pm 0.2$, and $\lambda' \simeq 2.2 \pm 0.4$ reported in Ref. [8]. While our approach uses the elastic energy, it is interesting to note that prior work on rigidity percolation has suggested the use of the number of floppy modes as a free energy [36].

Conclusion — The scaling theory and relations derived here for the strain- and connectivity-controlled rigidity transitions in athermal fiber networks are consistent with our numerical results, as well as prior results near the isostatic point [8–10]. Interestingly, for the subisostatic, strain-controlled transition, we observe that simulations of both triangular and packing-derived networks exhibit consistent non-mean-field exponents. This, together with agreement with the hyperscaling relation in Eq. (4) suggest that the upper critical dimension for fiber networks is $d_u > 2$, in contrast with jammed packings at the isostatic point [12]. Our observations, combined with prior evidence of similar exponents for alternate subisostatic network structures, including 2D and 3D phantom networks, honeycomb networks, and Mikado networks [11, 37], suggest that non-mean-field behavior might be ubiquitous in randomly-diluted subisostatic networks. Interestingly, the hyperscaling relation in Eq. (4), together with the observation that $f > 0$, suggests that fiber networks satisfy the Harris criterion [38], which would imply that such networks should be insensitive to disorder. Further work will be needed to test this hypothesis, as well as the scaling relations derived here in 3D.

[1] J. C. Maxwell, Philosophical Magazine **27**, 294 (1864).
[2] M. F. Thorpe, Journal of Non-Crystalline Solids **57**, 355 (1983).
[3] S. Feng and P. N. Sen, Phys. Rev. Lett. **52**, 216 (1984).

[4] M. E. Cates, J. P. Wittmer, J.-P. Bouchaud, and P. Claudin, Phys. Rev. Lett. **81**, 1841 (1998).

[5] A. J. Liu and S. R. Nagel, Nature **396**, 21 (1998).

[6] M. van Hecke, Journal of Physics: Condensed Matter **22**, 033101 (2010).

[7] M. Wyart, H. Liang, A. Kabla, and L. Mahadevan, Phys. Rev. Lett. **101**, 215501 (2008).

[8] C. P. Broedersz, X. Mao, T. C. Lubensky, and F. C. MacKintosh, Nature Physics **7**, 983 (2011).

[9] M. Das, D. A. Quint, and J. M. Schwarz, PLoS ONE **7**, e35939 (2012).

[10] J. Feng, H. Levine, X. Mao, and L. M. Sander, Soft Matter **12**, 1419 (2016).

[11] A. Sharma, A. J. Licup, K. A. Jansen, R. Rens, M. Sheinman, G. H. Koenderink, and F. C. MacKintosh, Nature Physics **12**, 584 (2016).

[12] C. P. Goodrich, A. J. Liu, and J. P. Sethna, Proceedings of the National Academy of Sciences **113**, 9745 (2016).

[13] W. G. Ellenbroek, E. Somfai, M. van Hecke, and W. van Saarloos, Phys. Rev. Lett. **97**, 258001 (2006).

[14] S. Alexander, Physics Reports **296**, 65 (1998).

[15] M. Sheinman, C. P. Broedersz, and F. C. MacKintosh, Phys. Rev. E **85**, 021801 (2012).

[16] A. Sharma, A. J. Licup, R. Rens, M. Vahabi, K. A. Jansen, G. H. Koenderink, and F. C. MacKintosh, Phys. Rev. E **94**, 042407 (2016).

[17] B. Widom, J. Chem. Phys. **43**, 3898 (1965).

[18] S. B. Lindström, A. Kulachenko, L. M. Jawerth, and D. A. Vader, Soft Matter **9**, 7302 (2013).

[19] H. J. Maris and L. P. Kadanoff, American Journal of Physics **46**, 652 (1978).

[20] M. Das, F. C. MacKintosh, and A. J. Levine, Phys. Rev. Lett. **99**, 038101 (2007).

[21] C. S. O'Hern, L. E. Silbert, A. J. Liu, and S. R. Nagel, Phys. Rev. E **68**, 011306 (2003).

[22] S. Dagois-Bohy, B. P. Tighe, J. Simon, S. Henkes, and M. van Hecke, Phys. Rev. Lett. **109**, 095703 (2012).

[23] C. P. Goodrich, A. J. Liu, and S. R. Nagel, Phys. Rev. Lett. **109**, 095704 (2012).

[24] See Supplemental Material for simulation details, κ-dependent nonaffinity data, and reanalyzed data from prior work, which includes Refs. [39–44].

[25] B. P. Tighe, Phys. Rev. Lett. **109**, 168303 (2012).

[26] Note that κ refers to the dimensionless bending stiffness $\kappa \equiv \kappa_b/(\mu l_c^2)$, in which κ_b is the bending rigidity used in the simulations and l_c is the average bond length in the unstrained network, $l_c = \langle l_{ij,0} \rangle$, with $l_c = l_0 = 1$ for triangular networks and $l_c \approx 1.03$ for packing-derived networks.

[27] A. W. Lees and S. F. Edwards, Journal of Physics C: Solid State Physics **5**, 1921 (1972).

[28] E. Bitzek, P. Koskinen, F. Gähler, M. Moseler, and P. Gumbsch, Phys. Rev. Lett. **97**, 170201 (2006).

[29] M. Doi and S. F. Edwards, *The Theory of Polymer Dynamics* (Clarendon Press, 1988).

[30] R. G. Larson, *The Structure and Rheology of Complex Fluids* (Oxford University Press, New York, 1999).

[31] M. F. J. Vermeulen, A. Bose, C. Storm, and W. G. Ellenbroek, Physical Review E **96**, 053003 (2017).

[32] M. Merkel, K. Baumgarten, B. P. Tighe, and M. L. Manning, Proceedings of the National Academy of Sciences (2019), 10.1073/pnas.1815436116.

[33] Interestingly, the values of f for these two systems appear to be consistent. It is unclear whether the difference between the corresponding values of ϕ is significant.

[34] R. Rens, C. Villarroel, G. Düring, and E. Lerner, Phys. Rev. E **98**, 62411 (2018).

[35] C. P. Broedersz, *Mechanics and dynamics of biopolymer networks*, Ph.D. thesis, Vrije Universiteit, Amsterdam (2011).

[36] D. J. Jacobs and M. F. Thorpe, Phys. Rev. Lett. **75**, 4051 (1995).

[37] R. Rens, M. Vahabi, A. J. Licup, F. C. MacKintosh, and A. Sharma, The Journal of Physical Chemistry B **120**, 5831 (2016).

[38] A. B. Harris, J. Phys. C: Solid State Phys **7**, 1671 (1974).

[39] *The Boost Graph Library: User Guide and Reference Manual* (Addison-Wesley Longman Publishing Co., Inc., Boston, MA, USA, 2002).

[40] N. C. Admal and E. B. Tadmor, Journal of Elasticity **100**, 63 (2010).

[41] T. J. Delph, Modelling and Simulation in Materials Science and Engineering **13**, 585 (2005).

[42] T. Ishikura, T. Hatano, and T. Yamato, Chemical Physics Letters **539-540**, 144 (2012).

[43] Y. Fu and J.-H. Song, The Journal of Chemical Physics **141**, 54108 (2014).

[44] A. T. Fenley, H. S. Muddana, and M. K. Gilson, PLoS ONE **9**, e113119 (2014).